

LOCATION OF BED INTERFACE IN SETTLING SLURRY PIPE FLOW USING ERT

A Adler¹, A Sutherland² and R Kotze³

¹*Systems and Computer Engineering, Carleton University, Ottawa, Canada;* ²*Flow Process & Rheology Centre (FPRC), Cape Peninsula University of Technology (CPUT), PO Box 652, Cape Town 8001, South Africa;* ³*Incipientus Ultrasound Flow Technologies AB, SE-412 76, Göteborg, Sweden.*

Electrical Resistance Tomography (ERT) is a non-invasive technique that can be used to monitor settling slurry pipe flow. Two aspects of the imaging were investigated. Of initial interest was the selection of an appropriate image reconstruction algorithm. Using the EIDORS open-source tool set, various image reconstruction algorithms were evaluated and results indicate the best performing was a combination of the Laplace and GREIT algorithms. Next, a novel functional measure was developed, using auto-correlations of image pixel waveforms, to detect the interface of the settled bed. The results of this analysis appear to show a zone of instability corresponding to the bed/supernatant interface at different flow rates, suggesting a promising way of extracting additional useful information from the ERT measurements.

KEY WORDS: Temporal correlation, ERT images, settling slurry flow

1. INTRODUCTION

Electrical Resistance Tomography (ERT), is a relatively low-cost method to determine the dynamic state of the internal distribution of the contents of pipes in a non-destructive and non-intrusive manner (Pinheiro et al., 1998). The use of ERT in laboratory scale pipe flow are reported in Dickin and Wang (1996), Grootveld et al. (1998), Vauhkonen et al. (1999), Tapp et al. (2003), Hartov et al. (2005) and Queiroz (2012). These authors all concluded that ERT is a promising technique to visualise slurry flow in a pipe. Giguère et al. (2008) conducted a successful study to identify homogeneous and heterogeneous slurry flow regimes, using image reconstructions and direct interpretation of ERT measurements.

In ERT, images are reconstructed to show the electrical conductivity (hence distribution) of material within the pipe, based on voltages measured at the internal surface of the pipe in response to an injected electrical current. It is a two-step process, requiring solution of the forward problem, followed by solution of the non-linear, ill-posed inverse problem (Adler and Boyle (2017)). The images are created via specific, selected reconstruction algorithms, the choice of which will significantly influence the quality and accuracy of the resulting images. Information on the effectiveness and accuracy of various image reconstruction algorithms is needed because ERT is susceptible to electrical noise and has relatively low spatial resolution, in addition to the ill-posedness of the inverse problem (Barber (2005), Zhang et al. (2011)). These limitations make it difficult to exploit

ERT images quantitatively. A systematic validation of ERT images of slurry flow is still necessary. Using the EIDORS software (Adler and Lionheart (2006)) Kotze et al. (2019) investigated the accuracy and suitability of different ERT reconstruction algorithms for settling slurry flow. Based on measurements made with a single concentration model slurry, for a limited number of flow rates and reconstruction parameters, they concluded that the Laplace or Laplace + GREIT algorithms gave the most accurate, consistent results.

To see if further useful information on coarse particle settling slurry flow can be extracted from the ERT data, the measurements for the flow tests described in Kotze et al. (2019) were re-analysed. The Laplace reconstruction algorithm was used to create time sequenced images for each flow condition, from which pixel value time series were extracted. These were used in time delayed auto-correlation calculations to identify areas of unsteadiness in the pipe cross-section for each flow condition.

2. EXPERIMENTAL APPARATUS AND MATERIALS

2.1 FLOW LOOP, ERT SPOOL PIECE AND ERT INSTRUMENT

The pipe loop used for the tests consisted of a $\varnothing 42.6$ mm PVC pipe, a Warman 2/1.5 inch rubber lined centrifugal pump controlled by a Yaskawa J1000 variable speed drive (VSD), a 160 l conical base mixing tank and a Krohne Optiflux 4000 electromagnetic flow meter (bulk flow rate). The ERT spool piece was made from non-conductive rigid polyvinyl chloride (PVC). It had two sets of electrode rings 5 cm apart, each with 16 stainless steel electrodes spaced equally around the inside circumference of the pipe (only one electrode ring used in this work). Observed flow rate was used to refer to identify (name) the different tests.

ERT measurements were made using 1 plane of the 8 measurement plane UCT ERT system (maximum of 1000 frames/sec). The hardware injects current across a pair of electrodes and measures the voltages on the other electrodes using the adjacent measurement strategy, to give 104 independent voltage measurements (effectively a spatial resolution of about 10% of pipe diameter). The instrument communicates with a PC for setup, to load and save the measured data and to display tomograms in real-time, using software developed at UCT. See Randall et al. (2005) and Wilkinson et al. (2006) for more details on the system.

3. EXPERIMENTS

The test slurry (mixture) comprised nominally $\varnothing 3$ mm black acetal beads, density 1.41 g/cm^3 (with some white beads to provide a visual aid) in a tap water/salt solution, which allowed easy creation of different flow regimes (e.g. stationary or sliding bed; heterogeneous or homogeneous flow). The actual concentration of beads was arbitrary and not determined for this work. Mixture temperature was $\sim 23 \pm 1$ °C. ERT data were acquired for 120 s for each test, at a frame rate of 566 Hz, and the average of every 25 frames was stored, resulting in approximately 2800 frames per measurement set. To compare bed depths estimated from the reconstructed images, photographs were taken.

Flow tests at four arbitrary bulk flow rates, namely 0.86 l/s, 1.30 l/s, 2.82 l/s and 4.50 l/s, referred to respectively as A, B, C & D, were done. Visual observations indicated that

at flow rate A there was a slowly sliding packed bed at the pipe invert with few beads suspended above it; at B a larger, less densely packed and faster sliding bed in the lower half of the pipe; at C a significant number of suspended beads with a visibly sheared (apparent concentration and velocity profiles through bed depth) sliding bed towards the pipe invert and at D largely heterogeneous flow (greater concentration of beads towards pipe invert, but no bed). See photographs in Figure 1.

4. ANALYSES AND RESULTS

4.1 IMAGE RECONSTRUCTIONS

Kotze et al. (2019) evaluated six selected ERT algorithms, namely Laplace, HPF, NOSER, Greit, TV-PDIPM and a combination of Laplace-GREIT, in the reconstruction of static objects and stationary and moving settled beds. For the moving beds (in terms of defined accuracy parameters) the Laplace algorithm performed best and was used to reconstruct the images used in the temporal analyses described in §4.2 (see Figure 1).

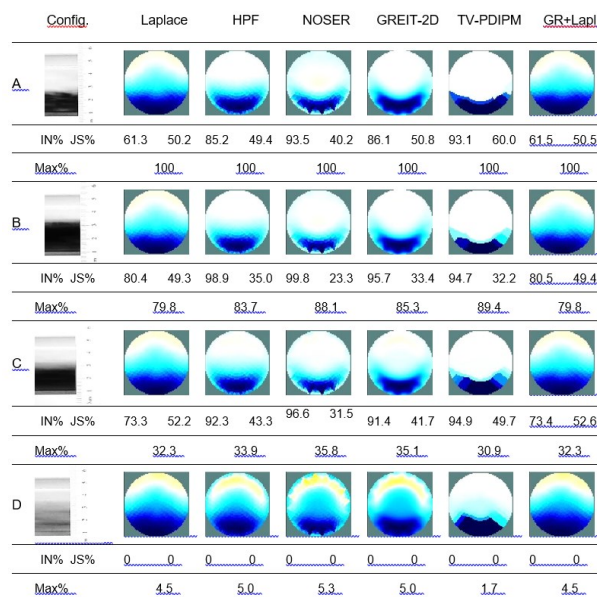


Figure 1. Bed levels (heights) and image reconstructions for the flow rates A (0.86 l/s) B (1.30 l/s) C (2.82 l/s) and D (4.50 l/s) [Kotze et al. (2019)]

4.2 TEMPORAL ANALYSIS OF FLOW TEST ERT MEASUREMENTS

When a slurry is flowing there can be a less precise interface between the settled bed and the fluid above it than when the slurry is static. Under steady flow conditions (as was the case for flows A to D) it seems reasonable to expect that the structure of the fluid/fluid-solids mixture in the “upper” part of the pipe and the “lower” part of the bed remain

reasonably consistent over time, and that they are separated by a transition region in which it may vary rapidly in size and concentration with time. With increasing flow rate this transition region is likely to become more unsteady and expand further across the pipe cross-section as the mixture becomes more heterogeneous. It can be expected that temporal correlation will be lower in the more unsteady regions, where the image pattern is likely to be more variable over time.

To investigate the validity of this assertion, for each of the flow conditions A to D, auto-correlations of time shifted image pixel waveforms extracted from a sequence of reconstructed images were calculated (block diagram in Figure 2). The expectation was that time delays over which the auto-correlation values are non-zero would give an indication of flow stability. The calculations were done as follows:

- for each measurement (frame of data) within a set an image was reconstructed using the Laplace algorithm, and stored in time sequence (approximately 40 ms apart)
- from these images a time series of pixel values was extracted for each pixel
- for each pixel time series, cross-correlations were calculated at 40 ms offsets from 0 to 120 s (correlation values are a maximum of 1 at time zero and decreases with increasing time delay)
- A value of 1 s was chosen as a threshold by which time any differences in the image (pixel values) would be apparent, and then for each pixel the maximum correlation value for delays > 1 s was found. This maximum value (always < 1) was set as the pixel value for a plot of correlation values across the pipe cross-section. Different threshold values were calculated and all resulted in similar images.

Selected results from analyses as described above for the four flow rates A (0.86 l/s), B (1.30 l/s), C (2.82 l/s) and D (4.50 l/s) are shown in Figure 3. The mA and frequency values in Figure 3 refer to the injection current level and VSD setting respectively.

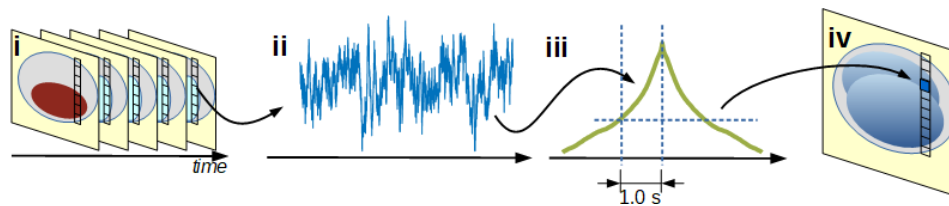


Figure 2. Block Diagram of showing the functional images of the time-series correlations. (i) raw image sequence, (ii) waveform of an individual pixel over time, (iii) auto-correlation of waveform (ii) and (iv) functional image of the normalized auto-correlation value at 1.0 s

The left column in Figure 3 shows the average ERT image, normalized to the maximum image (the image for the lowest flow rate). The centre column shows auto-correlations of time shifted pixel value waveforms at the indicated vertical positions (corresponding colours) on the average image centerline. The right column shows plots of pixel maximum auto-correlation values for time delays > 1 s. Darker parts of these plots show areas of lower temporal correlation. Note that in order not to mask any features in the data that the analyses might expose, the correlation plots for the different flow rates are to different scales.

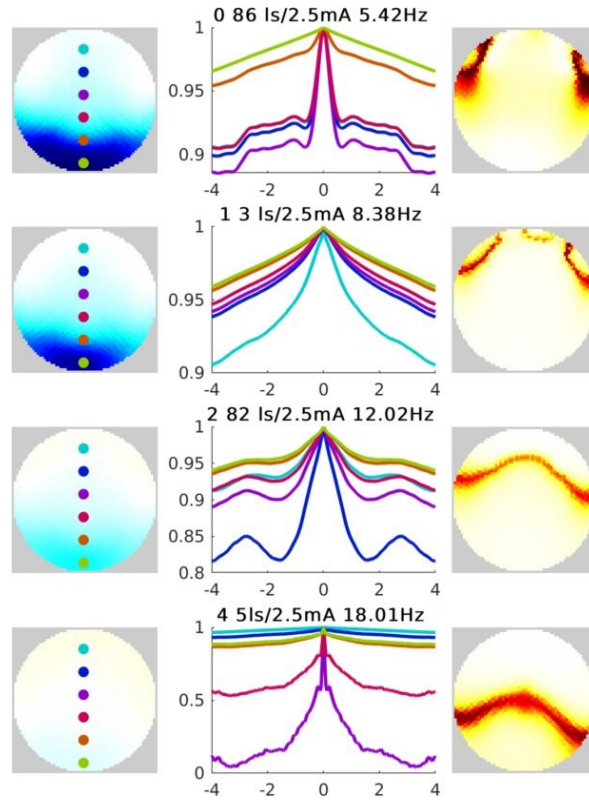


Figure 3. Average ERT images, selected cross-correlation plots and temporal correlation plots across pipe for bulk flow rates of A (0.86 l/s), B (1.30 l/s), C (2.82 l/s) and D (4.50 l/s) – 3 mm acetal beads in water

5. DISCUSSION

ERT is a promising technique for dynamic monitoring of solids in settling slurry pipe flow, but requires information on the accuracy and effectiveness of the image reconstruction techniques/algorithms used. This issue was addressed in Kotze et al. (2019), using a single concentration settling slurry (mixture) and a limited number of flow rates and image reconstruction parameters. The actual level of solids (bed height) in the images varies significantly with flow rate, since the conductivities of the settled bed and the supernatant become more similar with increasing flow rate, and ERT images of flowing settling slurries do not necessarily tell the whole story. For the flow conditions analysed, Kotze et al. (2019) introduced a parameter $Max\%$ (ratio of *Max pixel in current image*/*Max pixel over all images for flows A to D*) which is largely independent of the reconstruction algorithm. $Max\%$ is not a measure of the accuracy of the ERT image, but rather an indication of the relative difference in contrast between the highest and lowest density zones within the pipe. It decreased dramatically at the highest flow rate, in line with the

visual observation that the settled bed had disappeared. As Max% decreases the ERT image can be interpreted as representing a more heterogeneous to homogeneous flow of the mixture. However, as can be seen in Figure 1 the images from any given reconstruction algorithm for the different flow regimes look quite similar and an unsteady transition region is not obvious.

In an attempt to extract information on the transition zone, the dynamic components of the ERT images from the different flow rates were evaluated as described in §4.2. The left column of Figure 3 shows the average ERT images, normalised to the image at the lowest flow rate (maximum image). The images clearly indicate a diminishing bed with increasing flowrate. The first two images (for the flow rates 0.86 and 1.30 l/s) show the observed sliding bed, but suggest a distinct gradient in concentration across the height of the bed, which was not physically apparent. The ERT image for 2.82 l/s shows a definite region of increased concentration in the pipe invert, but suggests a much lower concentration and height than observed visually. The image at the highest flow rate of 4.50 l/s appears to be almost uniform, implying a highly heterogeneous to homogeneous distribution of the solids. The plots in the centre column of Figure 3 are of calculated auto-correlation values corresponding to the pixel positions (same colour coding) on the vertical centerline of the ERT images, shown for delays -4 to 4 s. Auto-correlation values are all a maximum at time delay zero, and drop off from there at varying rates, depending on position and flow regime. These plots clearly show greater correlation (less variance in image with time) towards the top and the invert of the pipe. The maximum values at every pixel position from auto-correlation calculations for delays > 1 s are shown in the images in the right column of Figure 3. These images have not been individually normalised so that any real features in each dataset can be “seen” in what would otherwise be almost uniform images (the high flow rate, heterogeneous images).

Looking at the auto-correlation values and their plots for the 0.86 and 1.30 l/s flow rates, no unsteady transition region is apparent, in agreement with the visual observations, but in contrast to what the ERT images might suggest. Temporal cross-correlation values over the whole pipe cross-section are high, showing that the flow is stable. The small regions of lower (but still high) correlation at approximately the 10 and 2 o'clock positions in the images for these flow rates are real features in the data, but the reason for their existence is not understood now. The image for flow at 2.82 l/s is uniform across the pipe cross-section except for a relatively small “horizontal” band of “unsteady” flow which has lower correlation values. This is in agreement with visual observations, in which a narrow (transition) band with a large number of particles was seen to be travelling faster than the settled particles below them, in which the particles are neither settled or fully suspended. The image is similar at 4.50 l/s, but the band showing much lower temporal correlation is broader and lower in the pipe. This could not be confirmed visually as there was no bed as such and the particles were travelling too fast to see. It is, however, physically plausible since as the flow rate increases more particles will be suspended, leaving fewer settled (smaller bed height) and the mixing region (particles swapping between “bed” and supernatant) will increase as the flow becomes more heterogeneous.

Although more research is necessary over a broader range of particle sizes, densities, flow rates and carrier fluids to understand what these “functional” images show, the

temporal correlation analyses of ERT image pixel waveforms appears to be a useful way to get more information from the time-series of ERT data.

6. CONCLUSION

The aim of this work was to see if reconstructed ERT images, in addition to representing the distribution of coarse solid particles in settling slurry pipe flows, also contain useful information on the thickness and location of the bed/supernatant transition zone. The assertion was that in the regions of the pipe outside the unsteady (mixing) transition zone the structures of the suspension are steady. The parts of the ERT images corresponding to these regions will vary little with time and therefore have high temporal correlation compared to the transition region. The Laplace algorithm was used to reconstruct ERT images from 120 s of measurements made with 3 mm acetal beads in water in a $\varnothing 42.6$ mm PVC pipe under different flow conditions. The images are about 40 ms apart, representing a frame rate of approximately 23 fr/s. Temporal correlation analyses of pixel value time series for each measurement set showed areas of steady and unsteady flow which largely agreed with visual observations and were physically plausible. Although considerably more research is needed to fully prove the validity of this type of analysis and to understand features of the data it reveals, initial results given here show it may be a useful way to extract additional information from ERT data.

ACKNOWLEDGEMENTS

The Cape Peninsula University of Technology (CPUT), Cape Town, South Africa, is acknowledged for funding.

REFERENCES

1. A Adler, A Boyle, "Electrical Impedance Tomography: Tissue Properties to Image Measures", *IEEE Trans Biomed Eng.* 64:2494–2504, 2017
2. A Adler, W.R.B. Lionheart, "Uses and abuses of EIDORS: an extensible software base for EIT. *Physiological Measurement*, 27(5), pp.S25-S42. 2006
3. Barber, D. C. 2005. EIT: The view from Sheffield. *Electrical impedance tomography: methods, history and applications*, DS Holder, Ed, 348-371.
4. Dickin, F., & Wang, M. 1996. Electrical resistance tomography for process applications. *Measurement Science and Technology*, 7(3), 247.
5. Giguère, R. Fradette, L. Mignon, D. Tangy, P.A., 2008. Characterization of slurry flow regime transitions by ERT. *Chemical Engineering Research and Design* 86, 989-996.
6. Grootveld, C. J., Segal, A., & Scarlett, B. 1998. Regularized modified Newton-Raphson technique applied to electrical impedance tomography. *International journal of imaging systems and technology*, 9(1), 60-65.
7. Hartov, A., Soni, N., & Halter, R. 2005. Breast cancer screening with electrical impedance tomography. *Electrical Impedance Tomography: Methods, History and Applications*, 167-185.
8. Kotze, R., Adler, A., Sutherland, A. & Deba, C. 2019. Evaluation of Electrical Resistance Tomography imaging algorithms to monitor settling slurry pipe flow. *Flow Measurement and Instrumentation*, Volume 68, August 2019, (101572).
9. Pinheiro, P.A.T., Loh, W.W. & Dickin, F.J., 1998. Three-dimensional reconstruction algorithm for electrical resistance tomography. *Science Measurement and Technology*, IEE Proceedings – Volume: 145, Issue: 3, 85 – 93.

10. Queiroz, J.L.L. 2012. Influence of regularization in image reconstruction in electrical impedance tomography. In *Journal of Physics: Conference Series* (Vol. 407, No. 1, pp. 012006). IOP Publishing, December 2012.
11. Randall, E. W., Wilkinson, A. J., Long, T. M., & Collins, A. 2005. The design of a flexible multi-layer ERT system and an evaluation of its performance. In *4th World Congress on Industrial Process Tomography*, Aizu, Japan.
12. Tapp, H.S., Peyton, A.J., Kemsley, E.K., & Wilson, R.H. 2003. Chemical engineering applications of electrical process tomography. *Sensors and Actuators B: Chemical*, 92(1), 17-24.
13. Vauhkonen, P.J., Vauhkonen, M., Savolainen, T., & Kaipio, J.P. 1999. Three-dimensional electrical impedance tomography based on the complete electrode model. *Biomedical Engineering, IEEE Transactions on*, 46(9), 1150-1160.
14. Wilkinson, A. J., Randall, E. W., Long, T. M., & Collins, A. 2006. The design of an ERT system for 3D data acquisition and a quantitative evaluation of its performance. *Measurement Science and Technology*, vol. 17, no. 8, pp. 2088-2096.
15. Zhang L., Wang H., Xu, Y. & Wang D. 2011. A Fast Iterative Shrinkage-Thresholding Algorithm for Electrical Resistance Tomography. *WSEAS Transactions on Circuit and Systems* 11, Vol10.